Controllable Scattering of a Single Photon inside a One-Dimensional Resonator Waveguide

Lan Zhou (周兰),[1,2] Z. R. Gong (龚志瑞),[3] Yu-xi Liu (刘玉玺),[1,4] C. P. Sun (孙昌璞),[3] and Franco Nori (野理)[1,4,5]

[1]*Advanced Science Institute, The Institute of Physical and Chemical Research (RIKEN), Wako-shi 351-0198, Japan*

[2]*Department of Physics, Hunan Normal University, Changsha 410081, China*

[3]*Institute of Theoretical Physics, The Chinese Academy of Sciences, Beijing, 100080, China*

[4]*CREST, Japan Science and Technology Agency (JST), Kawaguchi, Saitama 332-0012, Japan*

[5]*Center for Theoretical Physics, Physics Department, Center for the Study of Complex Systems, The University of Michigan, Ann Arbor, Michigan 48109-1040, USA*

(Received 27 February 2008; published 2 September 2008)

We analyze the coherent transport of a single photon, which propagates in a one-dimensional coupled-resonator waveguide and is scattered by a controllable two-level system located inside one of the resonators of this waveguide. Our approach, which uses discrete coordinates, unifies low and high energy effective theories for single-photon scattering. We show that the controllable two-level system can behave as a quantum switch for the coherent transport of a single photon. This study may inspire new electro-optical single-photon quantum devices. We also suggest an experimental setup based on superconducting transmission line resonators and qubits.

DOI: 10.1103/PhysRevLett.101.100501 PACS numbers: 03.67.Lx, 03.65.Nk, 85.25.−j

Introduction.—The scattering of a structureless particle can be used to determine the internal structure of a scattering target. This has been well recognized since the Rutherford experiments which ushered in modern particle and nuclear physics [1]. When scattering is confined to low dimensions, it displays new features. For example, the low-energy scattering of cold atoms confined in an atomic waveguide can form a gas of impenetrable bosons exhibiting total reflection [2]. Such total reflection, and related phenomena, motivate us to study low-dimensional photonic scattering, oriented towards quantum information processing, specifically, how to control the coherent transport of a scattered single photon by tuning the inner structure of the target so that the target can behave as a quantum switch, i.e., either a perfect mirror totally reflecting photons, or an ideal transparent medium allowing photons to pass. Based on theoretical studies of photonic scattering in one-dimensional (1D) waveguides [3], an all-optical single-photon transistor was recently proposed [4] by using surface plasmons confined in a conducting nanowire.

Here we study a quantum switch that controls the transport of a confined single photon. The switch is a scattering target made of a controllable two-level system. Our approach recovers the interesting results obtained via an effective field theory [3] in the "high" energy regime. Furthermore, it can also be consistently applied to the "low" energy regime discussed below. We show that the total reflection by a controllable two-level system can be realized as a resonant-scattering phenomenon and the reflection spectrum goes beyond the Breit-Wigner [1] and Fano line shapes [5,6].

As an application of our study, we propose an experimentally-accessible quantum electro-optical device, constructed using superconducting transmission line resonators [7–9] and a superconducting charge qubit [10–12]. In our proposed device, the scattering target is a charge qubit with two energy levels controlled by a gate voltage and an external magnetic flux; the coupled-transmission-line resonators behave as a 1D continuum for the coherent transport of photons. Thus, the controllable charge qubit can be used to manipulate the coherent transport of photons in an array of superconducting transmission line resonators.

Discrete scattering equation.—We consider a 1D coupled-resonator [13] waveguide (CRW) (see Fig. 1) with a two-level system, which is embedded in one of the resonators. The CRW can be realized by using either coupled superconducting transmission line resonators [14] or defect resonators in photonic crystals [15]. Let $a_j^\dagger$ ($j = -\infty, \cdots, \infty$) be the creation operator of the jth single-mode cavity with frequency ω. The Hamiltonian for the

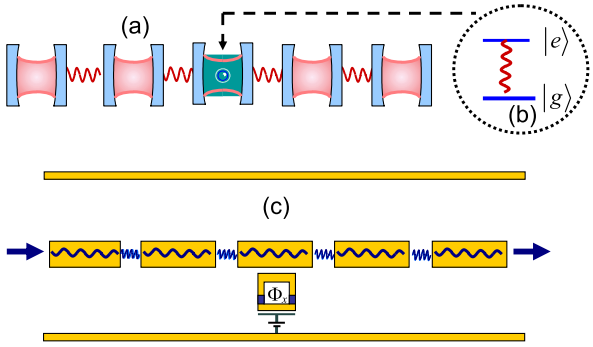

FIG. 1 (color online). Schematic configuration for the coherent transport of a single photon in a coupled-resonator waveguide (a) coupled to a two-level system (b), which is located in one of the resonators. (c) Schematic diagram of coupled superconducting transmission line resonators with one resonator coupled to a dc-SQUID-based charge qubit.

CRW is given by

$$H_c = \omega \sum_j a_j^\dagger a_j - \xi \sum_j (a_j^\dagger a_{j+1} + \text{H.c.}) \quad (1)$$

with the intercavity coupling constant ξ, which describes photon hopping from one cavity to another. Here, we assume that all resonators have the same frequency ω and $\hbar = 1$. The Hamiltonian (1) describes a typical tight-binding boson model, which has the dispersion relation $\Omega_k = \omega - V_k$, with $V_k = 2\xi \cos(lk)$. Below, the lattice constant l is assumed to be unity. In the low-energy regime, corresponding to *long wavelengths* ($\lambda \gg l$), the spectrum is quadratic: $\Omega_k \simeq \omega_\xi + \xi k^2$, with $\omega_\xi = \omega - 2\xi$. At the *matching condition* ($\lambda \sim 4l$), the spectrum is linear: $\Omega_k \simeq \omega_\xi \pm 2\xi k$. In contrast to the similar configurations in Refs. [16–19], here only one two-level system, with ground state $|g\rangle$, excited state $|e\rangle$ and transition energy Ω, is located inside one of coupled cavities. Moreover, Refs. [16–18] use several approximations which we do not make here, making the treatment here more physical, since we have exact solutions. For convenience, we take the 0th cavity as the coordinate-axis origin and we also assume that a two-level system is located in this 0th cavity [20]. Under the rotating wave approximation, the interaction between the 0th cavity field and the two-level system is described by a Jaynes-Cummings Hamiltonian

$$H_I = \Omega |e\rangle\langle e| + J(a_0^\dagger |g\rangle\langle e| + |e\rangle\langle g| a_0), \quad (2)$$

with the coupling strength J.

To study the 1D single-photon elastic scattering described by the total Hamiltonian $H = H_c + H_I$, we assume the stationary eigenstate

$$|\Omega_k\rangle = \sum_j u_k(j) a_j^\dagger |0\rangle|g\rangle + u_e |0\rangle|e\rangle, \quad (3)$$

when a single photon comes from the left with eigenenergy Ω_k. Here, $|0\rangle$ is the vacuum state of the cavity field, and u_e is the probability amplitude of the two-level system in the excited state. This $H|\Omega_k\rangle = \Omega_k|\Omega_k\rangle$ results in the discrete scattering equation

$$(V_k + JG_k\delta_{j0})u_k(j) = \xi[u_k(j+1) + u_k(j-1)]. \quad (4)$$

Here, the Green function $G_k = G_k(\Omega) = J/(\Omega_k - \Omega)$, and $u_e = G_k u_k(0)$ relates the excited-state amplitude u_e with the single-photon amplitude $u_k(0)$.

Reflection and transmission amplitudes.—Equation (3) presents a complete set of stationary states of the total system for single-photon processes. The scattering equation $V_k u_k(j) = \xi[u_k(j+1) + u_k(j-1)]$ for $j \neq 0$ has the solution

$$u_k(j) = \begin{cases} u_{Lk}(j) = e^{ikj} + re^{-ikj}, & j < 0 \\ u_{Rk}(j) = se^{ikj}, & j > 0 \end{cases} \quad (5)$$

with transmission and reflection amplitudes s and r. The continuous condition $u_k(0^+) = u_k(0^-)$ and the eigenvalue equation $(V_k + JG_k)u_k(0) = \xi[u_k(1) + u_k(-1)]$ at $j = 0$ determine the reflection amplitude

$$r = J^2[2i\xi \sin k(\omega - \Omega - 2\xi \cos k) - J^2]^{-1} \quad (6)$$

and the transmission amplitude s, with the constraints $s = r + 1$ and $|s|^2 + |r|^2 = 1$.

As shown below, Eq. (6) is a very useful result. Figures 2(a) and 2(c) show the reflection coefficient $R(k) = |r(k)|^2$ versus the momentum k of the incident photons, while Figs. 2(b) and 2(d) plot the reflection coefficient $R(\Delta) = |r(\Delta)|^2$ versus the detuning $\Delta = \Omega_k - \Omega$. Figure 2(b) represents a Breit-Wigner-like line shape around the resonance $\Delta = 0$, where the line width is proportional to J^2. At the resonance, the photon is completely reflected and the single two-level system behaves as a *perfect mirror*. Therefore, when the two-level system has a tunable transition energy, it can be used as a quantum switch to control the coherent transport of photons.

Because of the nonlinear dispersion relation $\Omega_k = \omega - 2\xi \cos k$, $|r(k)|^2$ in Figs. 2(a) and 2(c) shows a more general line shape, *beyond* the Breit-Wigner [1] and Fano [5] line shapes. Indeed, Eq. (6) is very general as it can directly provide results in different physical limits. When $|\Delta| < |\delta_\xi|$, as shown in Fig. 3, the generalized Fano-like line shape of the reflection spectrum

$$R(\Delta) = \frac{\eta(1 + \Delta/\delta_\xi + \Delta^2/\delta_\xi^2)}{(\Delta/\delta_\xi + y_0)^2 + \Gamma^2} \quad (7)$$

is approximately obtained from Eq. (6). Here, $\eta = J^4(J^4 - 4\xi\delta_\xi^3)^{-1}$, the detuning $\delta_\xi = \omega - \Omega - 2\xi$, $y_0 = \eta/2$, and $\Gamma^2 = \eta(1 - \eta/4)$.

When $\lambda \sim 4l$, the Breit-Wigner line shape [1]

$$r = -iJ^2[2\xi(\omega_\pi - \Omega \pm 2\xi k) + iJ^2]^{-1} \quad (8)$$

is also straightforwardly obtained from Eq. (6) by expand-

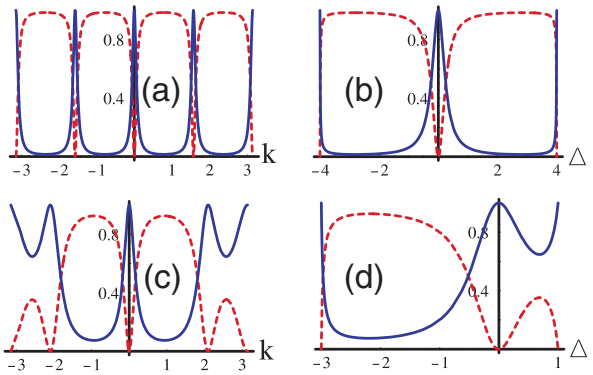

FIG. 2 (color online). The reflection coefficient R (blue solid line) and the transmission coefficient, $1 - R$ (red dashed line) as a function of either the momentum k or the detuning $\Delta = \Omega_k - \Omega$, when $\omega = \Omega = 5$ with intercavity coupling $\xi = 2$, [for (a), (b)]; and $\omega = 5$, $\Omega = 6$ with $\xi = 1$ [for (c),(d)]. Parameters are in units of J.

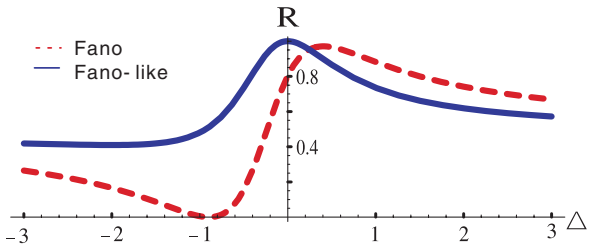

FIG. 3 (color online). Comparison between the Fano-like line shape (blue solid line) in Eq. (7) and the Fano line shape (red dashed line) given by $F(\Delta) = (\Delta/\delta_\xi + y_0 - q\Gamma)^2 \times [(\Delta/\delta_\xi + y_0)^2 + \Gamma^2]^{-1}$ at $\delta_\xi = -3$ and $\xi = 0.01$, where all the parameters are in units of J. The detunings are $\Delta = \Omega_k - \Omega$ and $\delta_\xi = \omega - \Omega - 2\xi$.

ing the cosine around $k = \pm\pi/2$, where $\omega_\pi = \omega - \pi\xi$. Equation (8) was also derived from the continuous field theory in Ref. [3]. Indeed, in this limit ($\lambda \sim 4l$), the Hamiltonian H_c for the CRW can be approximated by $H_c = \sum_j(\omega_\pi \pm 2\xi k)a_k^\dagger a_k$, producing a linear dispersion relation as in Ref. [3].

Low-energy effective theory.—Let us now consider the *long-wavelength regime* ($\lambda \gg l$) and use the low-energy effective theory to consistently describe the scattering of the confined photons. In this regime, k is so small that $\cos k \simeq 1 - k^2/2$, and $\sin k \simeq k$; thus, Eq. (6) becomes

$$r \simeq -iJ^2[2k\xi(\xi k^2 + \omega_\xi - \Omega) + iJ^2]^{-1}. \tag{9}$$

The result in Eq. (9), obtained from Eq. (6), can also be explained using the low-energy effective field theory described by the effective Hamiltonian

$$H = \int_{-\infty}^{\infty} dx\varphi^\dagger(x)(\omega_\xi - \xi\partial_x^2)\varphi(x) + \Omega|e\rangle\langle e| + \int_{-\infty}^{\infty} dxJ\delta(x)[\varphi^\dagger(x)|g\rangle\langle e| + \text{H.c}]. \tag{10}$$

Here, the field operator $\varphi(x) \equiv \int_{-\infty}^{\infty} dk \exp(ikx)a_k$ satisfies the commutation relation $[\varphi(x), \varphi^\dagger(x')] = \delta(x - x')$. Equation (10) can be derived from the momentum space representation of the total Hamiltonian

$$H = \sum_{k=0}^{N-1} \Omega_k \hat{a}_k^\dagger \hat{a}_k + \Omega|e\rangle\langle e| + \sum_{k=0}^{N-1}\left(\frac{J\hat{a}_k^\dagger}{\sqrt{N}}|g\rangle\langle e| + \text{H.c.}\right) \tag{11}$$

with $\Omega_k = \omega_\xi + \xi k^2/2$.

We now study single-photon scattering by a two-level system using the effective field theory in Eq. (10). Let us consider one photon, with energy Ω_k, incident from the left. The elastic scattering analysis assumes the stationary state $|\Omega_k\rangle = \int_{-\infty}^{\infty} dx u_k(x)\varphi^\dagger(x)|0\rangle|g\rangle + u_e|0\rangle|e\rangle$. Here, the conservation of total excitation $\sum_k n_k + |e\rangle\langle e| = 1$ is used. The eigenequation $H|\Omega_k\rangle = \Omega_k|\Omega_k\rangle$ provides a system of equations for the single-photon probability amplitudes $u_k(x)$ and the excited-state population u_e, which results in a scattering equation with resonance pole

$$\xi\partial_x^2 u_k(x) = G_k\delta(x)u_k(0) + (\omega_\xi - \Omega_k)u_k(x). \tag{12}$$

Then the photon scattering can be described by Eq. (12), which can be solved by assuming $u_k(x) = \exp(ikx) + r\exp(-ikx)$, for $x < 0$, and $u_k(x) = s\exp(ikx)$, for $x > 0$. The reflection amplitude in Eq. (9) can be obtained from Eq. (12) with the boundary condition due to the δ-function

$$\xi\left[\frac{\partial}{\partial x}u_k(\epsilon) - \frac{\partial}{\partial x}u_k(-\epsilon)\right] = \frac{J^2 u_k(0)}{\Omega_k - \Omega} \tag{13}$$

and the continuity $u_k(\epsilon) = u_k(-\epsilon)$.

Physical implementation.—To demonstrate our theoretical results on the reflection and transmission line shapes beyond the Breit-Wigner and Fano line shapes, we now propose an experimentally accessible quantum device shown in Fig. 1(c), that uses superconducting transmission line resonators and a dc-SQUID-based charge qubit [7,9,10]. Here, the charge qubit acts as the scattering target, and its internal structure (e.g., the transition frequency) is controllable by both the voltage applied to the gate and the external flux through the SQUID loop. The coupled coplanar transmission line resonators, constructed by cutting the superconducting transmission line into N equal segments [14], provide the continuum for the coherent transport of photons. The coupling ξ between two neighboring transmission line resonators is realized via dielectric materials (it depends on the concrete coupling mechanism). Then the Hamiltonian of the coupled-resonator waveguide is the same as that in Eq. (1).

The energy eigenstates of the charge qubit [11,12] are defined by $|e\rangle = \cos(\theta/2)|0\rangle - \sin(\theta/2)|1\rangle$ and $|g\rangle = \sin(\theta/2)|0\rangle + \cos(\theta/2)|1\rangle$, with the transition frequency $\Omega = \sqrt{B_z^2 + B_x^2}$ for $\theta = \arctan(B_x/B_z)$. $|0\rangle$ and $|1\rangle$ are charge eigenstates representing the excess Cooper pairs on the superconducting island. The parameter $B_z = 4E_C(2n_g - 1)$, with the charging energy $E_C = e^2/2(C_g + 2C_J)$ and $n_g = C_g V_g/2e$, can be controlled by the voltage V_g applied to the gate capacitance C_g. Here C_J is the capacitance of the Josephson junction. The parameter $B_x = 2E_J\cos(\pi\Phi_x/\Phi_0)$, with the Josephson energy E_J, can be changed by the external magnetic flux Φ_x through the SQUID loop.

As in Ref. [9], we assume that the charge qubit is placed in the antinode of the single-mode quantized electric field in the transmission line resonator with length L. Therefore, the quantized voltage $V_q = (\hat{a} + \hat{a}^\dagger)\sqrt{\omega/(Lc)}$, induced by the quantized electric field, is also applied to the charge qubit via the gate capacitance C_g. Here ω is the frequency of the quantized field, c is the capacitance per unit length of the transmission line. The coupling strength $J = (e\sin\theta C_g/C_\Sigma)\sqrt{\omega/(Lc)}$ between the qubit and the resona-

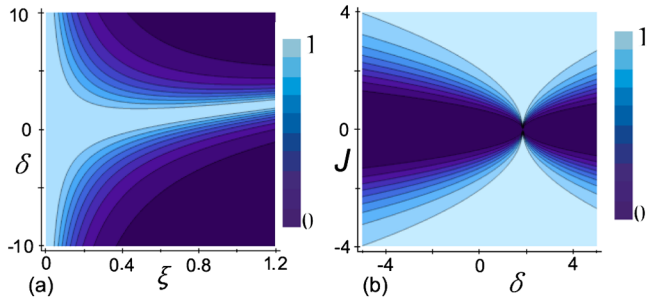

FIG. 4 (color online). Phase diagrams of the reflection spectrum $R(\Delta)$ in Eq. (7): (a) with respect to the intercavity coupling ξ and the detuning $\delta = \omega - \Omega$, in units of J; (b) with respect to J and δ, in units of ξ; both at $k = \pi/8$.

tor, with $C_\Sigma = C_g + 2C_J$, has feasible values in the range 5–200 MHz [9]. The detuning $\delta = \omega - \Omega$ between the charge qubit and the single-mode field can be changed from -10 to 10 GHz. The frequency of each resonator is in the range between 5–10 GHz, and the qubit frequency can be tuned from 5 to 15 GHz [9].

Using Eq. (6) and also the parameters given above, we can show that the scattering process of single-photon degenerates to a total reflection when the coupling strength ξ between the resonators vanishes or the incident photon resonates with the qubit. Also the stronger coupling between the qubit and the resonator corresponds to the larger reflection amplitude. The details of this phenomenon are depicted by the contour map of the reflection coefficient in Fig. 4. It can be regarded as a kind of phase diagram. In the white areas, the reflection is nearly one and the transmission is almost zero, while in the dark areas, the transmission approaches unity. The results obtained in this work are very different from previous quantum switches [21].

Conclusions.—We have studied the coherent transport of a single-photon confined in a 1D cavity array. The scattering target is a controllable two-level system. In the matching regime ($\lambda \sim 4l$), our approach recovers the results [3] obtained from its effective field theory. Our approach also predicts a general spectral structure in which the reflection and the transmission are beyond the usual Breit-Wigner and Fano line shapes. These results could be verified experimentally via a circuit QED system [7–9]. However, in reality, all large quantum systems interact with the environment, resulting in some inelastic scattering of photons. Thus the environment could affect the photon reflection coefficient, reducing the quantum switching efficiency. The environment-induced inelastic scattering is related to (i) the decoherence of the resonators; and (ii) the decay of the two-level system. Case (i) influences the free propagation of the single photon. The coherent scattering process happens only when the photon decay rate is much smaller than the intercavity coupling. Case (ii) broadens the width of the line shape at the resonance. Finally, we also note that the properties of the delivered photons at the end of the waveguide could be studied experimentally by measuring the transmission spectrum of the resonator.

This work is supported by NSFC No. 90203018, No. 10474104, No. 60433050, and No. 10704023, NFRPC No. 2006CB921205 and 2005CB724508. F. N. acknowledges partial support from the NSA, LPS, ARO, NSF grant No. EIA-0130383, JSPS-RFBR 06-02-91200, and the JSPS-CTC program.

[1] L. D. Landau and E. M. Lifshitz, *Quantum Mechanics (Nonrelativistic Theory)* (Butterworth, Boston, 1991).
[2] M. Olshanii, Phys. Rev. Lett. **81**, 938 (1998).
[3] J. T. Shen and S. Fan, Phys. Rev. Lett. **95**, 213001 (2005); J. T. Shen and S. Fan, *ibid.* **98**, 153003 (2007); Opt. Lett. **30**, 2001 (2005).
[4] D. E. Chang *et al.*, Nature Phys. **3**, 807 (2007).
[5] U. Fano, Phys. Rev. **124**, 1866 (1961).
[6] A. M. Satanin and Y. S. Joe, Phys. Rev. B **71**, 205417 (2005).
[7] J. Q. You and F. Nori, Phys. Rev. B **68**, 064509 (2003); J. Q. You, J. S. Tsai, and F. Nori, *ibid.* **68**, 024510 (2003).
[8] I. Chiorescu *et al.*, Nature (London) **431**, 159 (2004).
[9] A. Wallraff *et al.*, Nature (London) **431**, 162 (2004).
[10] M. A. Sillanpää *et al.*, Nature (London) **449**, 438 (2007).
[11] J. Q. You and F. Nori, Phys. Today **58**, No. 11, 42 (2005).
[12] G. Wendin and V. S. Shumeiko, arXiv:cond-mat/0508729.
[13] K. Yu. Bliokh, Yu. P. Bliokh, V. Freilikher, S. Savel'ev, and F. Nori, arXiv:0708.2653 [Rev. Mod. Phys. (to be published)].
[14] L. Zhou *et al.*, Phys. Rev. A **77**, 013831 (2008).
[15] A. Greentree *et al.*, Nature Phys. **2**, 856 (2006).
[16] L. Zhou *et al.*, Phys. Rev. A **76**, 012313 (2007).
[17] F. M. Hu *et al.*, Phys. Rev. A **76**, 013819 (2007).
[18] M. J. Hartmann *et al.*, Nature Phys. **2**, 849 (2006).
[19] A. L. Rakhmanov *et al.*, Phys. Rev. B **77**, 144507 (2008).
[20] If the coordinate-axis origin is not taken at the center of the cavity, where the two-level system is located, the reflection amplitude in Eq. (6) includes a position-dependent global phase.
[21] C. P. Sun *et al.*, Phys. Rev. A **73**, 022318 (2006); M. Mariantoni *et al.*, arXiv:0712.2522.